УДК 621.65 DOI 10.36910/775.24153966.2025.83.4

В. Ю. Кондусь

Сумський державний університет

ДОСЛІДЖЕННЯ РОБОЧИХ ХАРАКТЕРИСТИК ВІЛЬНОВИХРОВИХ НАСОСІВ ПРИ РОБОТІ У РОБОЧОМУ ДІАПАЗОНІ Q = 0,7-1,2 $Q_{ном}$

У роботі виконано чисельне дослідження робочих характеристик вільновихрового насоса СВН 80-32 у діапазоні подач Q = 0,7–1,2·Qном, що відповідає типовим умовам тривалої експлуатації насосного обладнання. На основі геометричних параметрів насоса побудовано тривимірні моделі та проведено CFD-аналіз у середовищі ANSYS CFX із застосуванням k–ε моделі турбулентності. Розглянуто два варіанти робочих коліс: з шістьма криволінійними лопатями та двоярусне колесо з дванадцятьма лопатями.

Отримані характеристики показали, що у робочому діапазоні обидва виконання забезпечують стабільний пологоспадний характер напірної кривої та близькі значення гідравлічного ККД (до 48,3% для шестилопатевого та 47,5% для двоярусного колеса). Водночас двоярусна система забезпечує приріст напору на 1,3–1,8 м (3–5%) без суттєвого зниження енергоефективності. Аналіз швидкісних і тискових полів показав, що двоярусне колесо формує більш рівномірне натікання на лопаті, зменшує дифузорність каналів та знижує вихрові втрати у вільній камері.

Результати дослідження дозволяють обґрунтувати вибір конструкції робочого колеса залежно від умов експлуатації: шестилопатеве виконання є більш доцільним у режимах, близьких до номінального, тоді як двоярусне забезпечує додатковий запас напору та кращу стабільність роботи у зонах підвищених подач.

Ключові слова: *вільновихровий насос; гідравлічні характеристики; CFD-аналіз; робочий діапазон подач; робоче колесо; двоярусна лопатева система; гідравлічний ККД; статичний тиск; швидкісні поля; енергетична ефективність.*

V. Kondus

INVESTIGATION OF THE OPERATIONAL CHARACTERISTICS OF TORQUE-FLOW PUMPS WITHIN THE OPERATING RANGE Q = 0.7–1.2 Q_{nom}

This study presents a numerical investigation of the operational characteristics of the torque-flow pump TFP 80-32 within the flow rate range Q = 0.7–1.2·Q_{nom}, which corresponds to typical conditions of long-term pump operation. Based on the geometric parameters of the pump, three-dimensional models were developed and a CFD analysis was carried out in ANSYS CFX using the k–ε turbulence model. Two types of impellers were considered: one with six curvilinear blades and a dual-tier impeller with twelve blades.

The obtained characteristics demonstrated that, within the operating range, both designs provide a stable, gently declining head curve and comparable hydraulic efficiency values (up to 48.3% for the six-blade impeller and 47.5% for the dual-tier impeller). At the same time, the dual-tier configuration ensures an increase in head by 1.3–1.8 m (3–5%) without a significant decrease in energy efficiency. Analysis of velocity and pressure fields showed that the dual-tier impeller provides more uniform flow distribution onto the blades, reduces channel diffusivity, and decreases vortex losses in the free chamber.

The results of the study justify the choice of impeller design depending on the operating conditions: the six-blade impeller is more suitable for regimes close to the nominal point, while the dual-tier impeller ensures an additional head margin and greater operational stability at higher flow rates.

Keywords: *torque-flow pump; hydraulic characteristics; CFD analysis; operating flow range; impeller; dual-tier blade system; hydraulic efficiency; static pressure; velocity fields; energy efficiency.*

1. Introduction

Torque-flow pumps have found wide application in industry and municipal utilities due to their ability to transport liquids containing solid and fibrous inclusions, as well as gas–liquid mixtures [1]. Their design features – simplified flow passage, presence of a free chamber, and minimal contact between the operating medium and the impeller – provide high reliability and resistance to clogging [2]. This makes torque-flow pumps competitive in cases where the operation of centrifugal counterparts is complicated.

At the same time, a key drawback of this pump type remains its relatively low efficiency (mainly 0.35–0.55) and limited head values. Therefore, selecting the optimal operating mode becomes crucial to ensure maximum efficiency under permissible operating conditions [3].

The nominal operating mode of a pump is generally determined by factory-specified values of flow rate and head. However, in real operating conditions, pumps most often operate in the range of 70 to 120% of the nominal flow rate [4]. This zone of operation is decisive for both the reliability of the equipment and the overall economy of the pumping process [5]. The insufficient amount of experimental data regarding the behavior of torque-flow pumps within the operating range Q = 0.7–1.2·Q_{nom} highlights the need for targeted investigations [6].

For ensuring stable and high-quality operation of pumping equipment, it is not enough to know the characteristics only at the optimal or nominal point. In practice, it is important to analyze pump behavior over a wider operating interval, where actual conditions often deviate from the rated parameters. It is within

© В. Ю. Кондусь

$Q = 0.7–1.2 \cdot Q_{nom}$ that most pumping regimes occur, determining their influence on the system's energy efficiency, reliability, and durability [7].

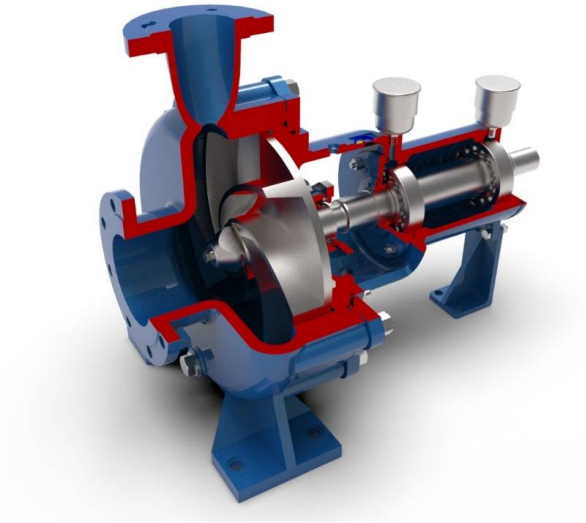

Fig. 1. **Structural design of a typical torque-flow pump of the TFP type**

The study of characteristics within this range makes it possible to identify not only the location of the maximum efficiency point but also the width of the operating zone where the pump maintains satisfactory hydraulic and energy performance. Such data are crucial for the selection of the drive motor, adjustment of control modes, and minimization of risks of overload or instability during operation [8].

Thus, the relevance of this work lies in modeling the head and energy characteristics of torque-flow pumps specifically within the operating flow range, which will refine recommendations for their application and provide a foundation for further optimization of their designs.

2. Literature review and formulation of the research problem.

Torque-flow pumps are considered in modern studies as an effective solution for pumping liquids with a high content of solid particles, fibrous inclusions, and gas admixtures [9, 10]. Due to their structural simplicity and reduced probability of clogging, they are widely used in municipal utilities, as well as in the food, chemical, and energy industries [11].

In recent years, researchers have focused on improving the flow passage and operating elements, which makes it possible to enhance the energy efficiency of such pumps [12]. In works [13, 14], new methods for designing impellers with a curvilinear blade profile and combined channels have been proposed, providing a reduction of hydraulic losses [15]. Both numerical simulations and experimental investigations of pump characteristics have been carried out, including the influence of design parameters on efficiency and head curves [16].

At the same time, most scientific works have focused on the optimization of operating elements or the analysis of hydrodynamic processes across a wide range of flow rates, including extreme regimes (0.2–0.4·Qnom and above 1.3·Qnom) [17]. Much less attention has been paid to the systematic study of characteristics specifically within the operating interval $Q = 0.7–1.2 \cdot Q_{nom}$, which is the most typical for long-term operation of pumping equipment [18].

Thus, the available literature confirms the importance of investigating torque-flow pumps but reveals a scientific gap associated with the insufficient amount of experimental data in the zone of real operating flow rates. Filling this gap will make it possible to more accurately determine the position of the maximum efficiency point, the width of the operating range, and the conditions for stable pump operation.

3. The aim and objectives of the research.

The aim of this work is to conduct a numerical investigation of the hydraulic and energy characteristics of torque-flow pumps within the operating flow range $Q = 0.7–1.2 \cdot Q_{nom}$ in order to refine the optimal conditions for their operation.

To achieve this goal, the following tasks were set:

1. To construct a three-dimensional model of the flow passage of the torque-flow pump.
2. To perform CFD simulations of pump operation at different flow rates within the range $Q = 0.7–1.2 \cdot Q_{nom}$.

© В. Ю. Кондусь

3. To determine the “head–flow rate” and “efficiency–flow rate” dependencies based on numerical results.
4. To identify the position of the maximum efficiency point and evaluate its deviation relative to the nominal flow rate.
5. To assess the width of the operating zone where the pump maintains satisfactory performance and to define its behavior outside the optimal regime.
6. To formulate practical recommendations for applying the results of numerical modeling in the further optimization of pump designs and their operation.

4. Research Methodology.

The initial data for modeling were the geometric parameters of the TFP 80-32 pump. Based on these, three-dimensional solid models of the impeller and the flow passage of the casing were created in SolidWorks (Fig. 2). Separate models were developed for the single-tier and double-tier impellers.

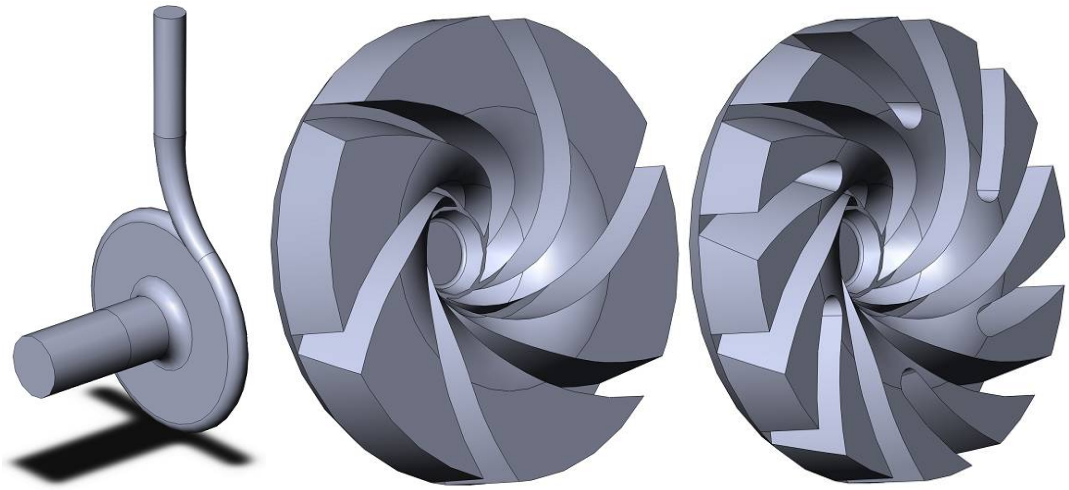

a b c

Fig. 2. **Models of the TFP 80-32 pump components (in SolidWorks): a – stator element of the casing; b – rotor element with a single-tier impeller; c – rotor element with a double-tier impeller**

The preparation of the computational domains was carried out in ANSYS ICEM CFD [19], where the stator (casing) and rotor (impeller) zones were generated independently. For each zone, an unstructured mesh with local refinement near the walls in the form of prismatic layers was created (Fig. 3). The total number of elements was about 1.45 million for the single-tier impeller model and up to 1.75 million for the double-tier model (Fig. 3b,c), ensuring a balance between accuracy and computational cost. The minimum mesh quality did not drop below 0.35–0.37.

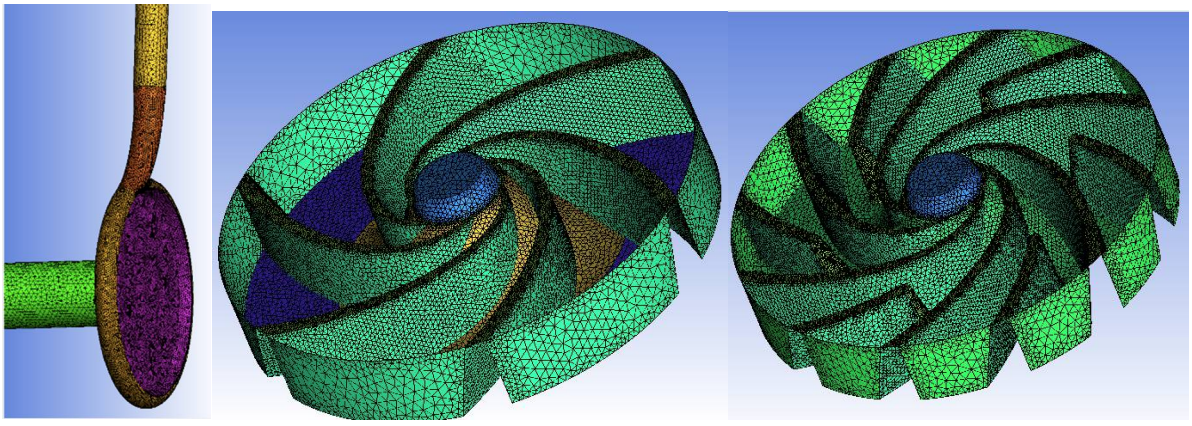

Fig.3. **Structure of the generated computational meshes: a – stator element of the casing; b – rotor element with a single-tier impeller; c – rotor element with a double-tier impeller**

© В. Ю. Кондусь

The meshes were then exported into ANSYS CFX-Pre, where the boundary conditions were specified (Fig. 4). At the inlet, a constant mass flow rate was defined, while at the outlet, a static pressure of 0.4 MPa was imposed. The simulations were carried out in a steady-state formulation using the k–ε turbulence model, which is a widely accepted approach for describing flows in torque-flow pumps. The interaction between rotor and stator domains was modeled using Frozen Rotor and Stage interfaces.

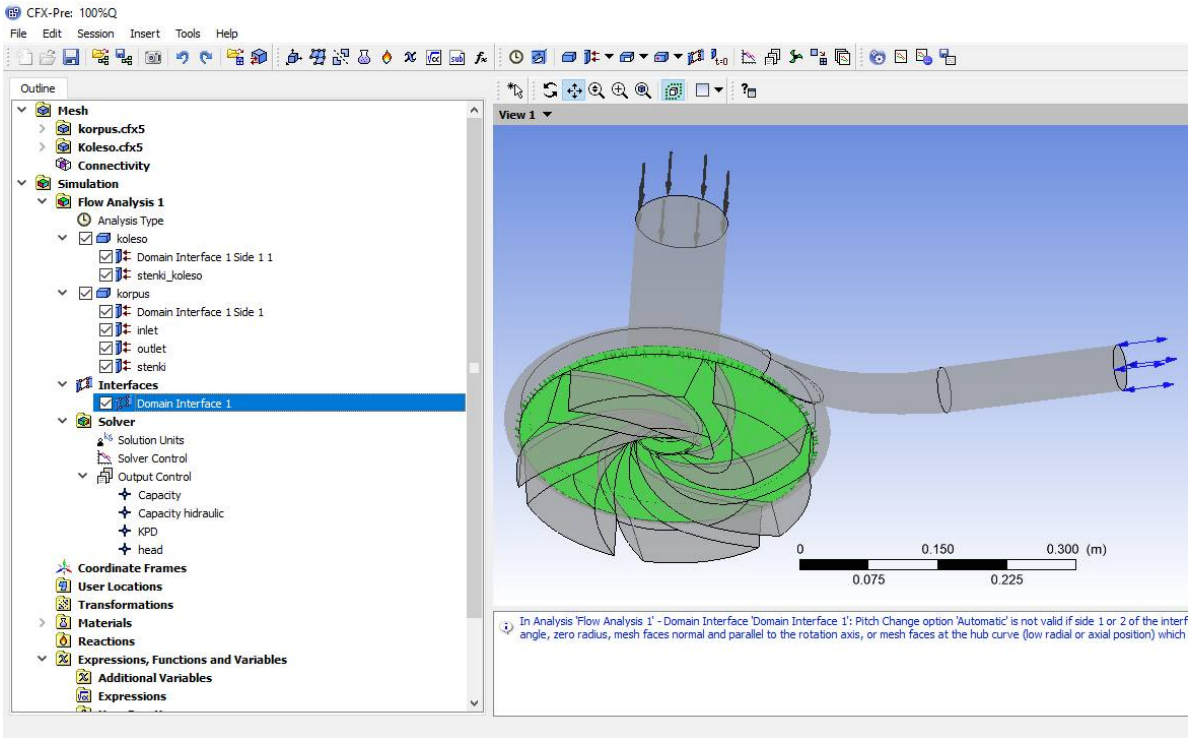

Fig. 4. **Boundary conditions applied in ANSYS CFX-Pre**

The study was conducted within the operating flow range Q = 0.7–1.2·Q_{nom}, which corresponds to practical long-term operating conditions of pumps [20, 21]. For the nominal flow rate (Q = Qnom = 80 m³/h, approximately 22.2 kg/s), baseline calculations were performed, while for other flow rates the mass flow was adjusted according to proportional relations. The surface roughness of the flow passage was set to 100 μm, corresponding to cast surfaces of the components.

The convergence criteria were defined as achieving a root-mean-square deviation of mass balance and torque not exceeding 10^{-4}. Additionally, head, hydraulic power, input power, and efficiency were monitored throughout the simulations.

5. Research Results.

The developed computational models and the adopted simulation parameters made it possible to perform a series of numerical studies in the operating flow range Q = 0.7–1.2·Q_{nom}. As a result, the main hydraulic and energy performance indicators of the pump were determined [22, 23], including the "head–flow" and "efficiency–flow" dependencies, as well as the position of the maximum efficiency point for two designs of the TFP 80-32 pump (Fig. 5): with a six-curved-blade impeller (blue line) and with a double-tier impeller of twelve blades (red line).

The modeling results and their analysis are presented below.

Numerical simulations (Fig. 5) showed that for both impeller configurations, the pump maintains stable head–flow curves and similar efficiency profiles. According to API 610, pumps are allowed to operate short-term within 70–120% Q_{nom} and long-term within 90–110% Q_{nom}. For the studied pump, this corresponds to flow ranges of 56–96 m³/h (short-term) and 72–88 m³/h (long-term).

The results indicate that the use of the double-tier impeller increases the head by 1.3 m (≈3.4%) at the best efficiency point (BEP), while the hydraulic and overall efficiency remain nearly identical between both configurations. This confirms the feasibility of using the improved impeller to boost head without reducing efficiency.

© В. Ю. Кондусь

In the operating flow range Q = 0.7–1.2·Q_{nom}, the head curve maintains a stable, gradually decreasing trend. At low flow rates (<0.5·Q_{nom}), a head "dip" is observed, which may cause flow instability; however, operation in this zone is not permitted by the standard.

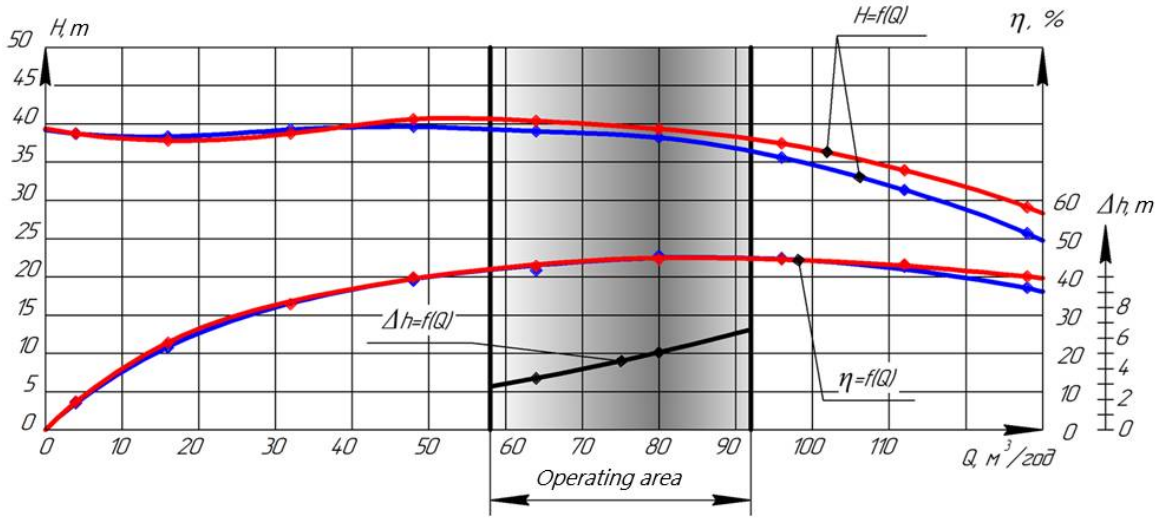

Fig. 5. **Characteristics of the TFP 80-32 pump with a six-curved-blade impeller (blue line) and a double-tier impeller with twelve blades (red line) in the operating range Q = 0.7–1.2·Q_{nom}.**

At the nominal flow (Q = Q_{nom} = 80 m³/h), the hydraulic efficiency reached 48.3% for the six-blade impeller and 47.5% for the double-tier impeller. The corresponding overall efficiency values were 45.5% and 44.6%. The difference between variants did not exceed the numerical error margin.

Tables 1 and 2 summarize the working parameters of the SVH 80-32 pump with both impeller configurations in the operating range.

Table 1.

Operating parameters of TFP 80-32 pump with six-blade impeller

Flow rate, % Q_{nom}	**60**	**70**	**80**	**90**	**100**	**110**	**120**
Flow rate, m³/h	48	56	64	72	80	88	96
Head, m	39,63	39.33	39.02	38.62	38.21	36.91	35.61
Hydraulic power, W	5184	6001	6805	7576	8330	8851	9316
Input power, W	12521	14005	15361	16363	17246	18440	19530
Hydraulic efficiency	0.414	0.429	0.443	0.463	0.483	0.480	0.477
Overall efficiency	0.39	0.404	0.417	0.436	0.455	0.452	0.449

Table 2.

Operating parameters of TFP 80-32 pump with double-tier impeller

Flow rate, % Q_{nom}	**60**	**70**	**80**	**90**	**100**	**110**	**120**
Flow rate, m³/h	48	56	64	72	80	88	96
Head, m	40.59	40.48	40.37	39.86	39.34	38.40	37.45
Hydraulic power, W	5309	6177	7041	7820	8576	9207	9797
Input power, W	12522	14055	15474	16816	18055	19404	20669
Hydraulic efficiency	0.424	0.440	0.455	0.465	0.475	0.475	0.474
Overall efficiency	0.399	0.414	0.428	0.438	0.447	0.447	0.446

A comparison of results showed that the double-tier impeller consistently increases head (by 3–5% within Q = 0.7–1.2·Q_{nom}) while maintaining nearly the same hydraulic and overall efficiencies. Meanwhile, the six-blade impeller has a slight advantage in peak efficiency (by up to 1%) at the nominal flow.

For operation in reduced flow zones (0.8–0.9·Q_{nom}), or where an additional head margin is required, the double-tier impeller is more advantageous. It provides a wider efficiency "plateau" and smoother head

© В. Ю. Кондусь

reduction at high flow rates, positively affecting system stability. If maximum energy efficiency at nominal flow is the priority, the six-blade design is preferable.

The maximum efficiency values reached about ηhyd = 0.48–0.49 and ηtot = 0.45–0.46. The difference between the two designs did not exceed 0.5–1%, within the bounds of numerical accuracy. In the range of 90–110% Qnom, the efficiency remained at least 95% of the peak, which defines the optimal long-term operating zone.

Thus, the double-tier impeller increases pump head without noticeable efficiency losses, making it preferable when additional head margin and stable energy performance are required. The choice of impeller type should therefore be based on operating conditions: the double-tier design suits variable flow regimes and high-head applications, while the six-blade impeller is better for stable operation near the nominal point.

Flow fields analysis.

Figure 6 presents the results of numerical simulation of the absolute velocity distribution in the flow passage and the central cross-section of the TFP 80-32 pump for two impeller configurations: with six blades and with a double-tier system of twelve blades. In both cases, the velocity fields exhibit a similar pattern, indicating the absence of significant differences in the overall flow structure.

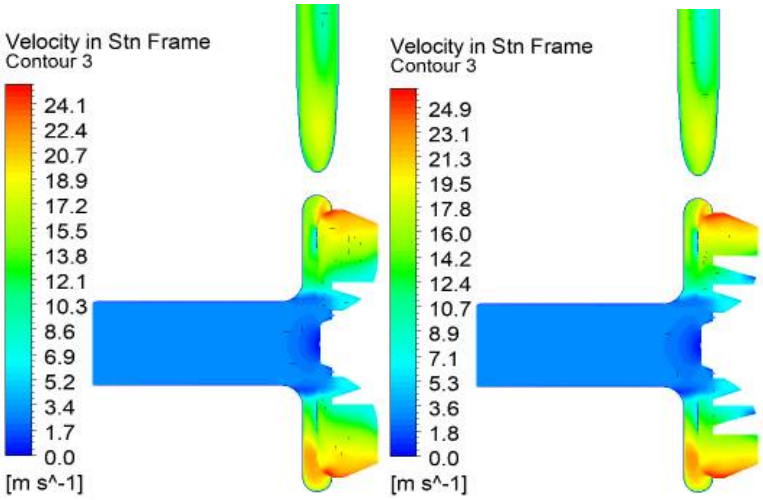

a b

Fig. 6. **Absolute velocity distribution in the central cross-section of the TFP 80-32 pump: a – with a six-blade impeller; b – with a double-tier impeller system.**

A similar picture is observed for the static pressure distribution (Fig. 7): in the central cross-section of the pump, the flow trajectories are practically identical. This suggests that, for qualitative analysis, it is sufficient to examine selected cross-sections, focusing on key differences in the inter-blade channel zone.

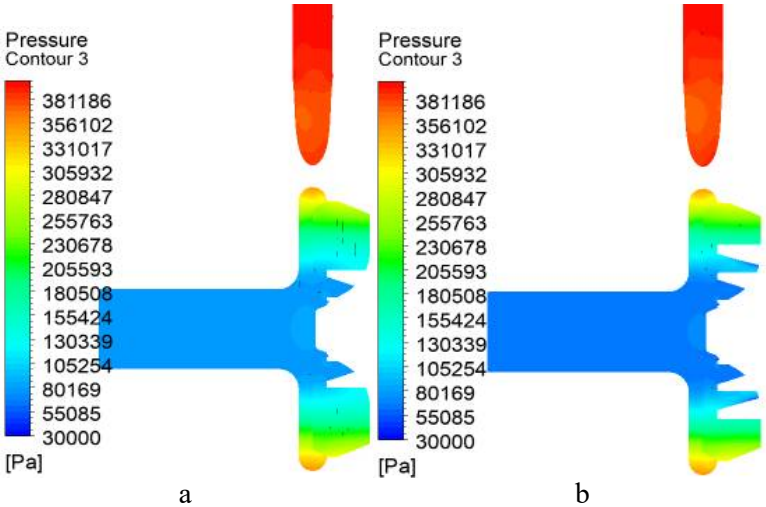

a b

Fig. 7. **Static pressure distribution in the central cross-section of the SVH 80-32 pump: a – with a six-blade impeller; b – with a double-tier impeller system**

© В. Ю. Кондусь

Operating Mode Q = Q_{nom} (80 m³/h).

Figures 8–10 show the distribution of relative velocity in the impeller flow channels (at the leading edge, in the central part, and near the disk) under the nominal operating mode (Q = Q_{nom}). For the six-blade impeller, excessive channel diffusivity is observed, leading to non-uniform flow incidence (areas of reduced velocity are highlighted in blue). In the case of the double-tier system, the flow formation is smoother and more uniform, which reduces losses and improves blade incidence.

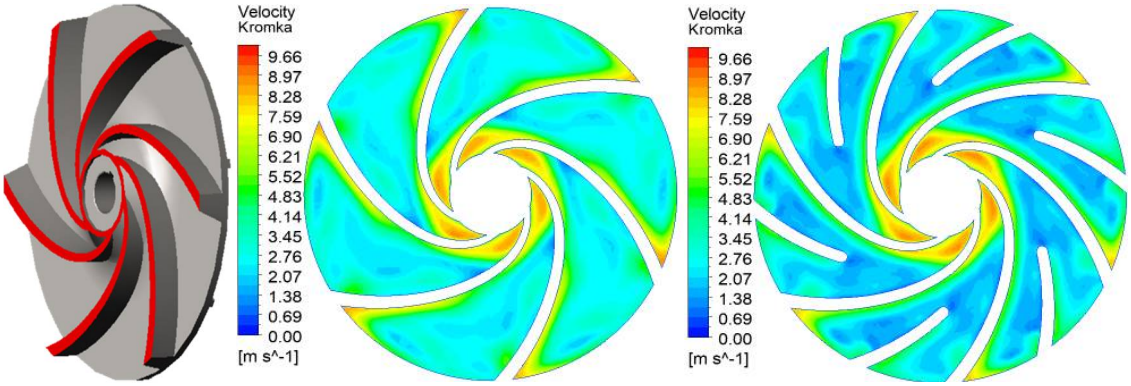

Fig. 8. **Distribution of relative velocity in the impeller flow channels at the leading edge (Q = Q_{nom}): a – cross-section location; b – six-blade impeller; c – double-tier impeller system**

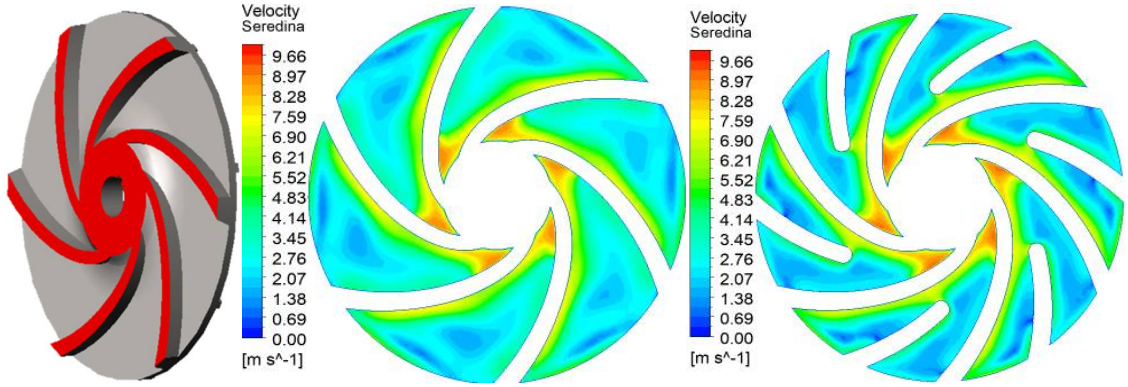

Fig. 9. **Distribution of relative velocity in the impeller flow channels at the midspan (Q = Q_{nom}): a – cross-section location; b – six-blade impeller; c – double-tier impeller system**

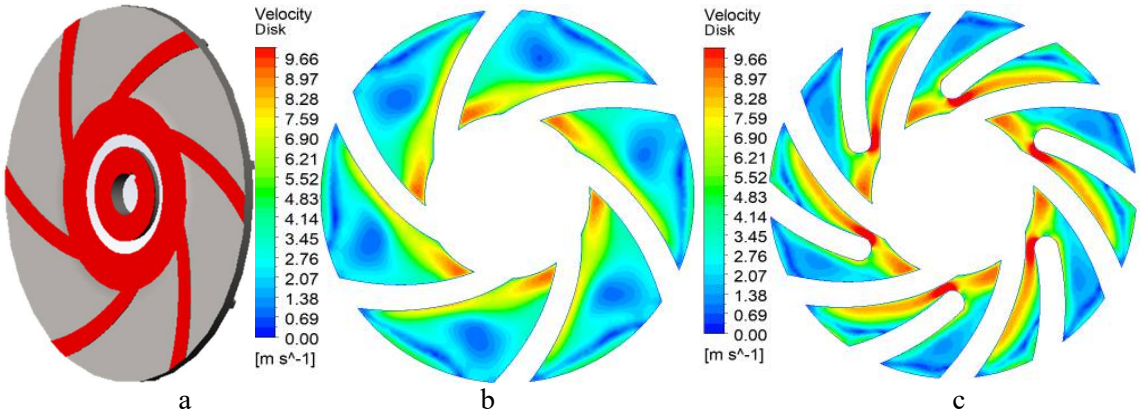

Fig. 10. **Distribution of relative velocity in the impeller flow channels near the disk (Q = Q_{nom}):**
a – cross-section location; b – six-blade impeller; c – double-tier impeller system

It should be noted that the use of an impeller with a large number of primary blades (without tier division) would lead to grid thickening near the hub, an increase in hydraulic resistance at the inlet, and intensification of vortex losses, which would negatively affect efficiency. The double-tier design helps to avoid this effect, while ensuring a more uniform distribution of velocities in the inter-blade channels.

© В. Ю. Кондусь

Operating Mode Q = 0.7·Qnom (56 m³/h)

Figures 11–13 present the results of numerical simulations of the relative velocity distribution in the impeller flow channels of the SVHN 80-32 pump at Q = 0.7·Qnom. The analysis was performed for three characteristic zones: at the blade leading edge, in the midspan of the channel, and near the impeller disk.

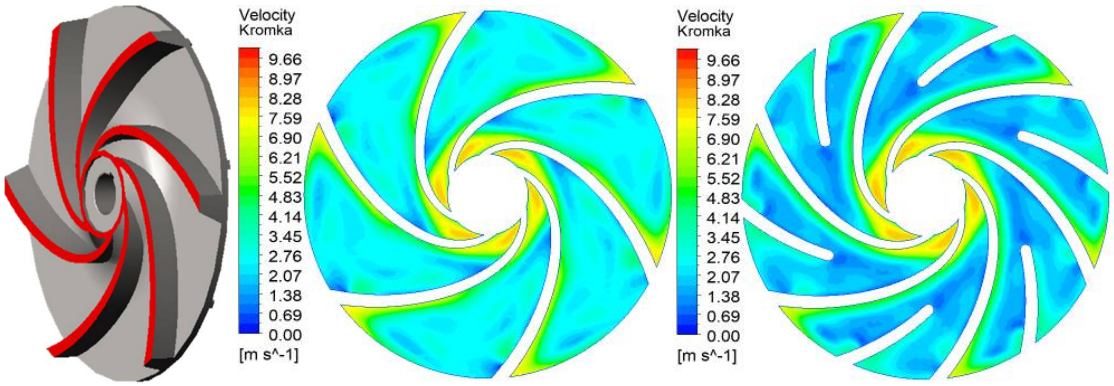

Fig. 11. **Distribution of relative velocity in the impeller flow channels at the leading edge ($Q = 0.7 \cdot Q_{nom}$): a – cross-section location; b – six-blade impeller; c – double-tier impeller system**

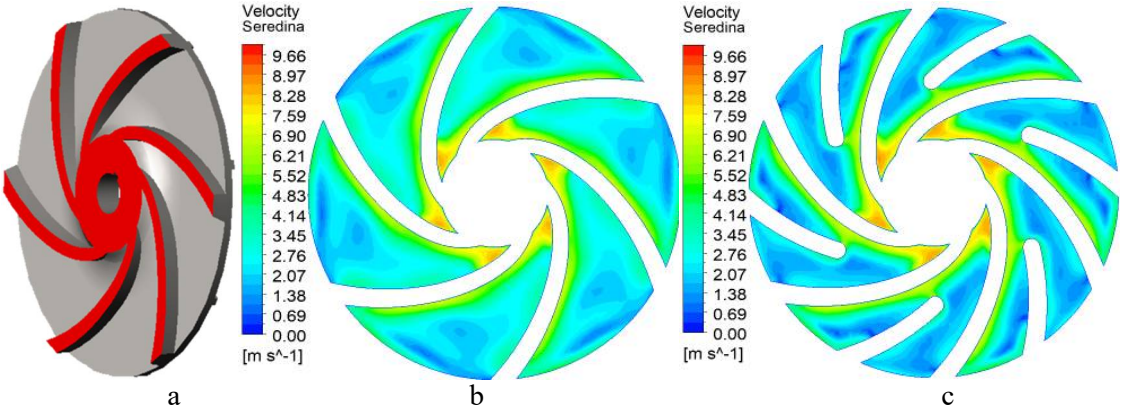

Fig. 12. **Distribution of relative velocity in the impeller flow channels at the midspan ($Q = 0.7 \cdot Q_{nom}$): a – cross-section location; b – six-blade impeller; c – double-tier impeller system**

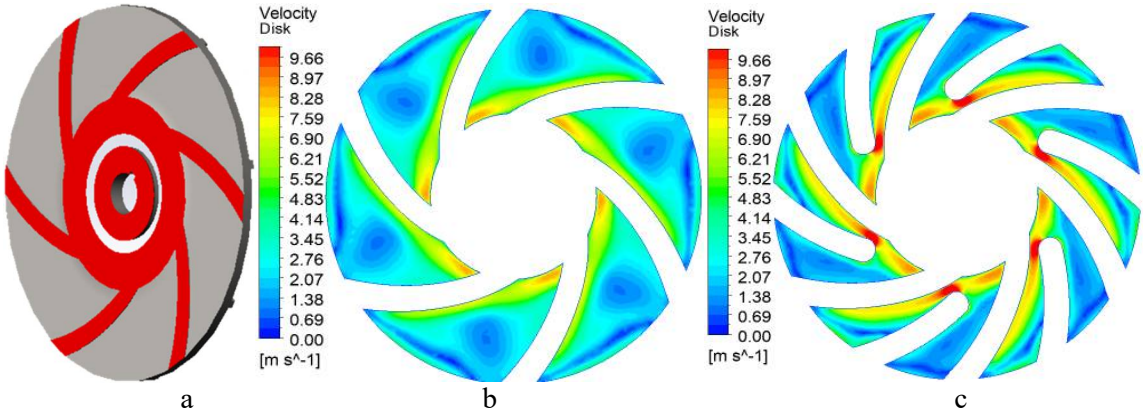

Fig. 13. **Distribution of relative velocity in the impeller flow channels near the disk ($Q = 0.7 \cdot Q_{nom}$): a – cross-section location; b – six-blade impeller; c – double-tier impeller system**

For the baseline six-blade design, noticeable channel diffusivity is observed, which results in zones of reduced velocity near the walls. This indicates less uniform flow incidence and can cause local hydraulic losses. In the case of the double-tier system, the velocity distribution is more uniform: the inlet flow passes over the blades more smoothly, while the velocity fields at the midspan and near the disk exhibit a more symmetrical pattern.

© В. Ю. Кондусь

A comparison with the nominal flow rate mode ($Q = Q_{nom}$) shows that the overall flow structure in the inter-blade channels remains similar. However, in the low-flow zone, the advantage of the double-tier impeller becomes more evident: due to lower diffusivity and a higher number of channels, the area of stagnant zones is reduced, which positively influences pump operating stability.

Thus, at $Q = 0.7 \cdot Q_{nom}$, the double-tier impeller provides a more rational distribution of relative velocities in the inter-blade channels. This confirms the earlier conclusion about the effectiveness of such a design specifically in the low-flow zone, where high efficiency is maintained along with an increase in head.

Operating Mode $Q = 1.2 \cdot Q_{nom}$ (96 m³/h).

Figures 14–16 present the relative velocity fields in the impeller flow channels of the SVHN 80-32 pump at Q = 1.2·Qnom. The analysis was carried out for three characteristic cross-sections: at the blade leading edge, in the midspan region, and near the impeller disk.

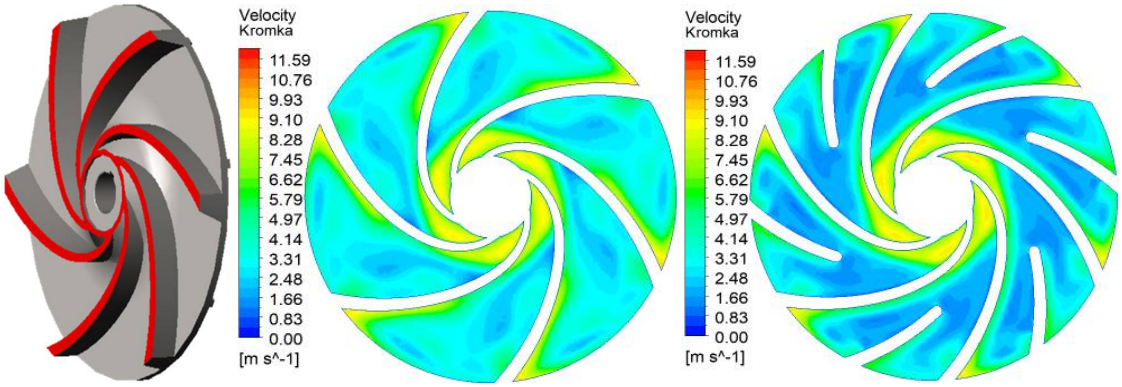

Fig. 14. **Distribution of relative velocity in the impeller flow channels at the leading edge ($Q = 1.2 \cdot Q_{nom}$): a – cross-section location; b – six-blade impeller; c – double-tier impeller system**

The comparison between the six-blade and the double-tier impellers shows that the overall flow structure remains similar to that of the optimal operating condition. However, at higher flow rates, the non-uniformity of velocity fields increases due to the higher discharge through the channels and the emergence of additional acceleration zones. For the six-blade impeller, this effect is more pronounced, manifesting as local regions of elevated velocity, which may lead to increased hydraulic losses.

In the case of the double-tier impeller, the relative velocity distribution is more balanced: even at high flow rates, the incidence on the blades remains relatively uniform, and no stagnant zones are formed. This is consistent with the head calculation results, where the double-tier configuration provides an additional head rise (up to 1.8 m, or more than 5% at Q = 1.2·Qnom).

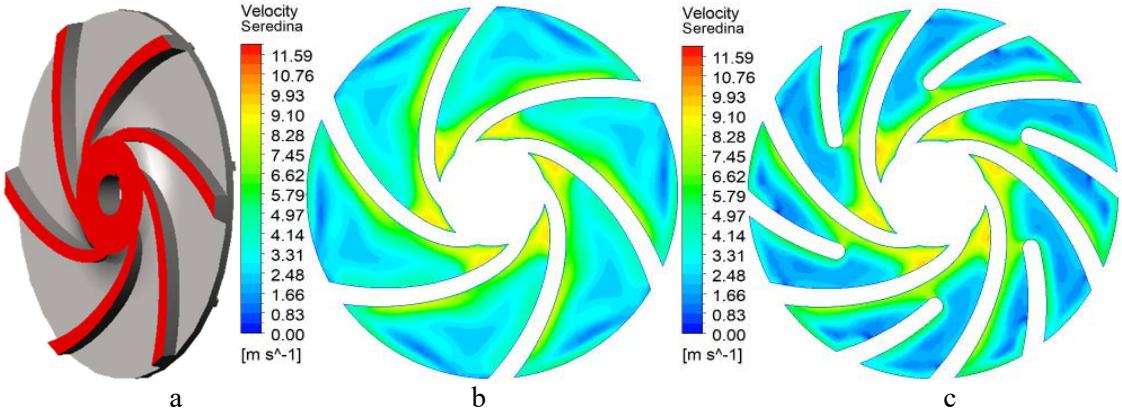

Fig. 15. **Distribution of relative velocity in the impeller flow channels at the midspan ($Q = 1.2 \cdot Q_{nom}$): a – cross-section location; b – six-blade impeller; c – double-tier impeller system**

Thus, at the upper boundary of the operating range (Q = 1.2·Qnom), the double-tier blade system demonstrates better flow stability and more efficient utilization of the flow passage. This makes such a configuration more suitable for operation under high-flow conditions, where an additional head margin is required while maintaining efficiency values close to the maximum.

© В. Ю. Кондусь

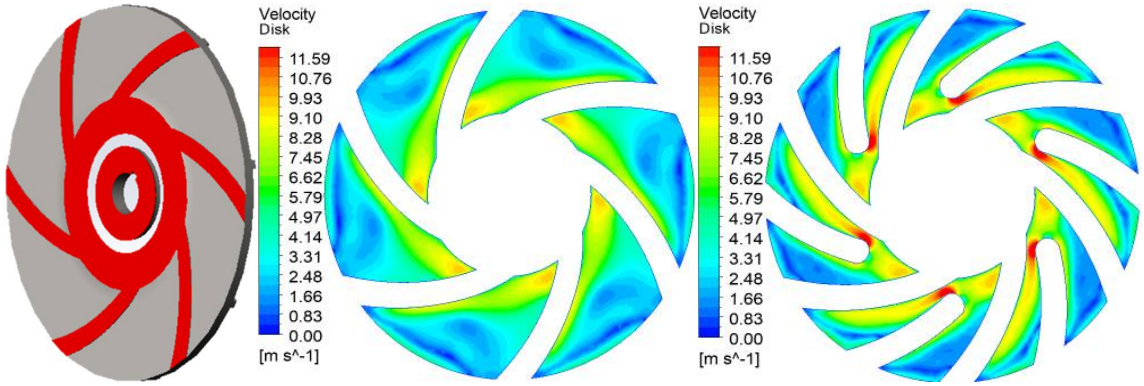

a b c

Fig. 16. **Distribution of relative velocity in the impeller flow channels near the disk ($Q = 1.2 \cdot Q_{nom}$): a – cross-section location; b – six-blade impeller; c – double-tier impeller system**

Flow Analysis in the Free Vortex Chamber

Further investigations concerned the distribution of static pressure and the components of absolute velocity (tangential Vu, axial Vz, and radial Vr) within the free vortex chamber of the TFP 80-32 pump. The calculations were performed in three characteristic zones: 5 mm from the casing wall, at the center of the free chamber, and near the blade edges.

Figure 17 presents the pressure fields, which correspond to the theoretically expected parabolic dependence on the reference radius. The obtained distribution is in full agreement with the fundamental equations of hydraulic machines, confirming the correctness of the CFD modeling.

The distribution of the tangential velocity component *Vu* (Fig. 18) also demonstrates the characteristic radial profile. At small radius ($R \approx 0.2R_2$), this component approaches zero, which corresponds to axial fluid inflow. The maximum values of *Vu* are observed near the outer diameter ($R = 0.8–1.0R_2$). The difference between the six-blade and the double-tier impellers is negligible, indicating a similar flow swirl structure.

Figure 19 shows the axial velocity component *Vz*, which clearly reflects the flow inlet and outlet regions. The inflow into the impeller occurs within the range $R = 0–0.4R_2$. In the double-tier configuration, the amount of fluid entering the impeller is approximately 10% higher than in the standard variant. The outflow occurs within $R = 0.6–1.0R_2$; for the double-tier impeller, the discharge is slightly higher, explained by the reduced share of the vortex component and the increased role of the blade-driven process.

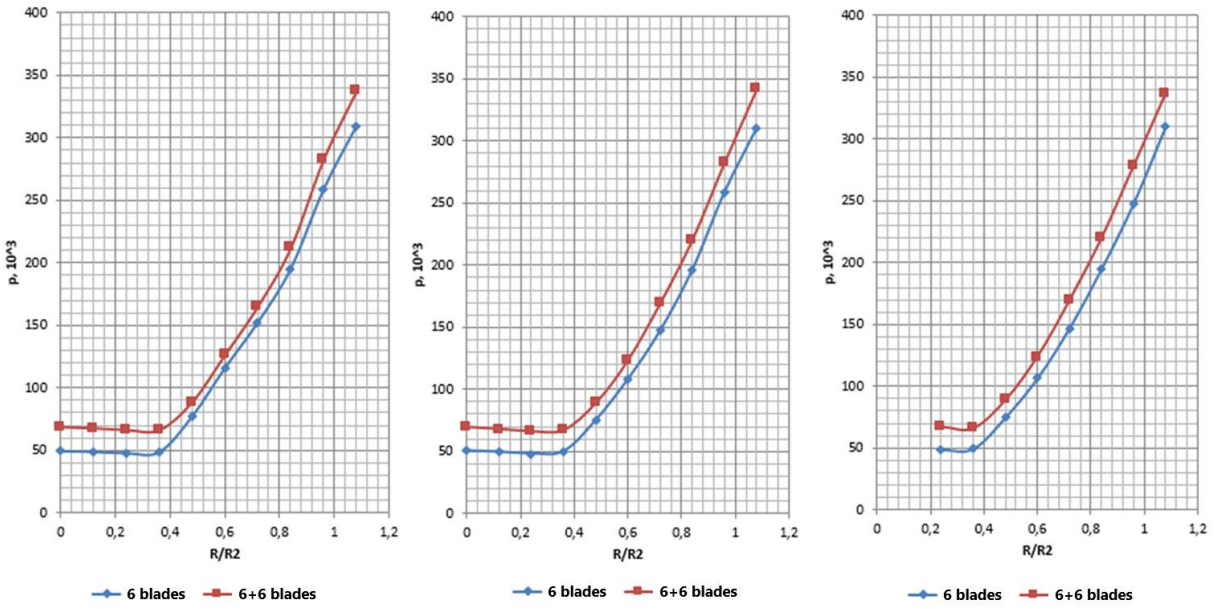

a b c

Fig. 17. **Pressure distribution in the free vortex chamber of the TFP 80-32 torque-flow pump: a – 5 mm from the casing wall; b – at the center of the chamber; c – 5 mm from the blade edge**

© В. Ю. Кондусь

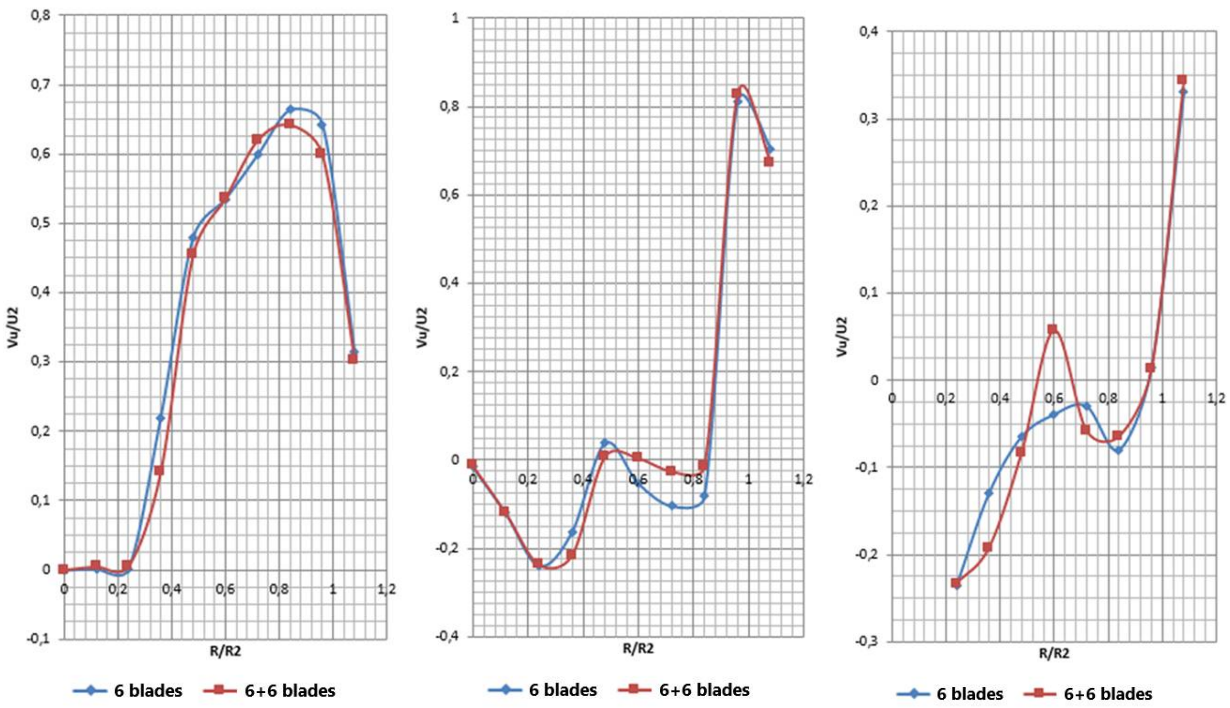

Fig. 18. **Distribution of the tangential component of absolute velocity *Vu* in the free vortex chamber of the TFP 80-32 torque-flow pump: a – 5 mm from the casing wall; b – at the chamber center; c – 5 mm from the blade edge**

The distribution of the radial velocity component *Vr* (Fig. 19) provides insight into the structure of the toroidal vortex [24] within the free chamber. The *Vr* values are somewhat higher for the double-tier impeller, which indicates a reduction in the intensity of the vortex-driven process and a greater involvement of the flow in the blade-driven mechanism.

Overall, the obtained results demonstrate that the double-tier blade system ensures more efficient utilization of the free vortex chamber, increases the share of blade-driven operation, and reduces vortex losses. This confirms its advantages compared to the standard six-blade impeller.

6. Conclusions

1. Based on the geometric parameters of the TFP 80-32 pump, solid models were developed and numerical simulations of the operating process were performed in ANSYS CFX. The applied methodology demonstrated good convergence of results and made it possible to obtain the complete characteristics of the pump across the entire operating flow range.

2. It was established that within the range $Q = 0.7–1.2 \cdot Q_{nom}$, the head characteristic has a stable, gradually decreasing trend, without signs of unstable operation. The hydraulic efficiency reaches 48.3% for the six-blade impeller and 47.5% for the double-tier impeller, which corresponds to the catalog values of pumps of this type.

3. The study showed that the use of the double-tier impeller provides a head increase of approximately 1.3 m (≈3.4% at $Q = Q_{nom}$ and up to 1.8 m at $Q = 1.2 \cdot Q_{nom}$) without significant efficiency losses. This confirms the feasibility of such a design in cases where an additional head margin is required.

4. The analysis of velocity fields in the inter-blade channels revealed that the six-blade configuration exhibits excessive channel diffusivity and uneven inflow, whereas the double-tier design ensures a smoother velocity distribution and reduces stagnant zones.

5. The investigation of the static pressure and velocity components (Vu, Vz, Vr) in the free vortex chamber confirmed that the double-tier blade system reduces vortex losses and increases the share of the blade-driven process. This improves flow stability and enhances pump efficiency across the entire operating flow range.

6. The obtained results provide the basis for practical recommendations regarding the application of torque-flow pumps with advanced impeller designs. They can also be used for further optimization of their construction in order to improve energy efficiency.

© *В. Ю. Кондусь*

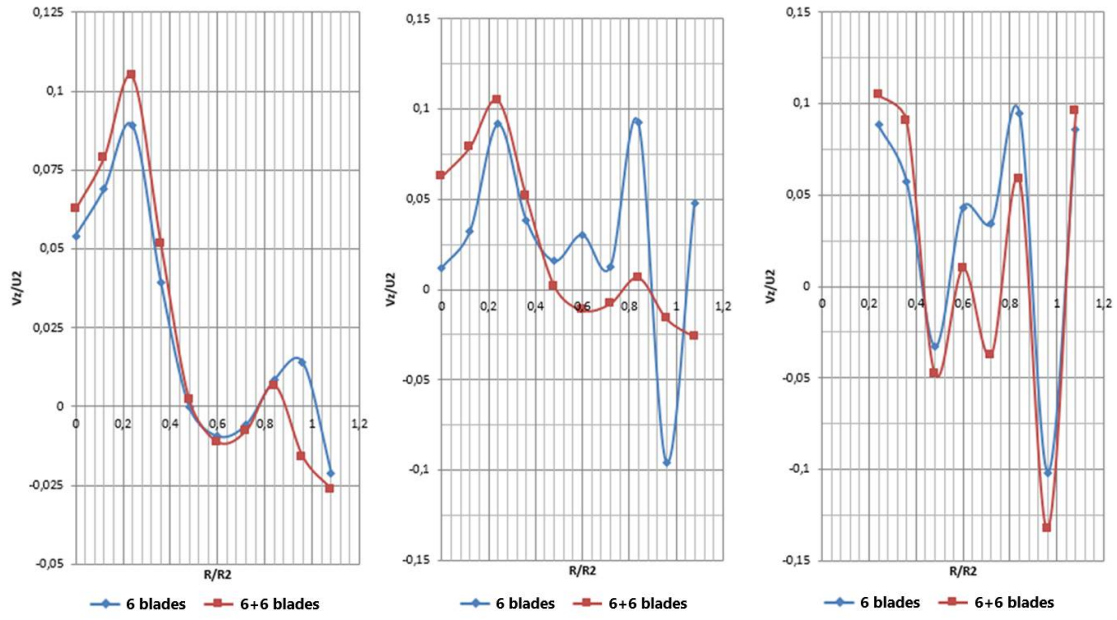

a b c

Fig. 19. **Distribution of the axial component of absolute velocity *Vz* in the free vortex chamber of the TFP 80-32 torque-flow pump: a – 5 mm from the casing wall; b – at the chamber center; c – 5 mm from the blade edge**

References:

1. Kotenko, A., Herman, V., Kotenko, A. (2014). Rationalization of Ukrainian industrial enterprises in a context of using torque flow pumps on the basis of valuation of the life cycle of pumping equipment. *Nauka i Studia*, Vol. 16 (126), pp. 83–91. http://essuir.sumdu.edu.ua/bitstream/123456789/38769/3/kotenko–poland1.PDF

2. Gusak, O., Krishtop, I., German, V., Baga, V. (2017). Increase of economy of torque flow pump with high specific speed. *IOP Conf. Ser.: Mater. Sci. Eng.,* 233 012004. Retrieved from https://doi.org/10.1088/1757-899X/233/1/012004

3. Antonenko, S., Sapozhnikov, S., Kondus, V., Chernobrova, A., Mandryka, A. (2021). Creation a universal technique of predicting performance curves for small-sized centrifugal stages of well oil pump units. *Journal of Physics: Conference series*, Vol. 1741 012011. https://doi.org/10.1088/1742-6596/1741/1/012011

4. Oliveira A., Ramirez J. Design of Pumping Installations with the Energy-Efficient Pumps (EEP) Tool. Energies, Vol. 18(16), 4248. Retrieved from https://doi.org/10.3390/en18164248

5. Dehnavi, E., Danlos, A., Solis, M., Kebdani, M., Bakir, F. (2024). Study on the pump cavitation characteristic through novel independent rotation of inducer and centrifugal impeller in co-rotation and counter-rotation modes. *Physics of Fluids*, Vol. 36(1), pp. 015120. Retrieved from http://dx.doi.org/10.1063/5.0182731

6. Quan, H., Chai, Y., Li, R., Guo, J. (2019). Numerical simulation and experiment for study on internal flow pattern of vortex pump. *Engineering Computations*, 36, 1579–1596. Retrieved from https://doi.org/10.1108/EC-09-2018-0420

7. Dehnavi, E., Solis, M., Danlos, A., Kebdani, M., Bakir, F. (2023). Improving the Performance of an Innovative Centrifugal Pump through the Independent Rotation of an Inducer and Centrifugal Impeller Speeds. *Energies*, 16(17), 6321. Retrieved from https://doi.org/10.3390/en16176321

8. Jung, D.-W., Seo, C.-W., Lim, Y.-C., ... Lee, S.-Y., Suh, H.-K. (2023). Analysis of Flow Characteristics of a Debris Filter in a Condenser Tube Cleaning System. *Energies*, 2023, 16(11), 4472 Retrieved from https://doi.org/10.3390/en16114472

9. Krishtop, I., German, V., Gusak, A., Lugova, S., & Kochevsky, A. (2014). Numerical Approach for Simulation of Fluid Flow in Torque Flow Pumps. In Applied Mechanics and Materials. *Trans Tech Publications, Ltd.*, 630, 43–51. Retrieved from https://doi.org/10.4028/www.scientific.net/amm.630.43

10.Gerlach, A., Thamsen, P. & Lykholt-Ustrup, F. (2016). Experimental Investigation on the Performance of a Vortex Pump using Winglets. *ISROMAC 2016. International Symposium on Transport*

Phenomena and Dynamics of Rotating Machinery. Retrieved from http://isromac-isimet.univ-lille1.fr/upload–dir/finalpaper/181.finalpaper.pdf

11.Krishtop, I. (2015). Creating the flowing part of the high energy-efficiency torque flow pump. *Eastern-European Journal of Enterprise Technologies*, 2 (74), 31–37. Retrieved from https://doi.org/10.15587/1729-4061.2015.39934

12.Dehghan, A., Shojaeefard, M., Roshanaei, M. (2024) Exploring a new criterion to determine the onset of cavitation in centrifugal pumps from energy-saving standpoint; experimental and numerical investigation. *Energies*, Vol. 293, 130681. Retrieved from http://dx.doi.org/10.1016/j.energy.2024.130681

13.Kondus, V., Kalinichenko, P., Gusak, O. (2018). A method of designing of torque-flow pump impeller with curvilinear blade profile. *Eastern-European Journal of Enterprise Technologies*, 3/8 (93), 29–35. Retrieved from https://doi.org/10.15587/1729-4061.2018.131159

14.Kondus, V., Puzik, R., German, V., Panchenko, V., Yakhnenko, S. (2021). Improving the efficiency of the operating process of high specific speed torque-flow pumps by upgrading the flowing part design. *Journal of Process Mechanical Engineering*, Vol. 237, pp. 1741 012023 https://doi.org/10.1088/1742-6596/1741/1/012023

15.Gao, X., Shi, W., Zhang, D., Zhang, Q. & Fang, B. (2014). Optimization design and test of vortex pump based on CFD orthogonal test. *Nongye Jixie Xuebao/Transactions of the Chinese Society for Agricultural Machinery*, 45 (5), 101–106. Retrieved from http://dx.doi.org/10.6041/j.issn.1000-1298.2014.05.016

16.Kumar, J., Gopi, S., Amirthagadeswaran, K. (2023). Redesigning and numerical simulation of gating system to reduce cold shut defect in submersible pump part castings. *Proceedings of the Institution of Mechanical Engineers, Part E: Journal of Process Mechanical Engineering*, Vol. 237 (3), pp. 971-981. https://doi.org/10.1177/09544089221142185

17.Panchenko, V., German, V., Ivchenko, O., Ryasnaya, O. (2021). Combined operating process of torque flow pump. *Journal of Physics: Conference series*, Vol. 1741 012011. Retrieved from https://doi.org/10.1088/1742-6596/1741/1/012022

18.Dehnavi, E., Bakir, F., Danlos, A., Kebdani, M. (2023). Numerical Analysis of Distance Effect between Inducer and Centrifugal Impeller in Independent Rotational Turbopump in Co-rotating and Counter-rotating Mode. *European Conference on Turbomachinery Fluid Dynamics and Thermodynamics, ETC*, 2023. Retrieved from http://dx.doi.org/10.29008/ETC2023-203

19.Dehnavi, E., Bakir, F., Danlos, A., Kebdani, M. (2023). Numerical Analysis of Distance Effect between Inducer and Centrifugal Impeller in Independent Rotational Turbopump in Co-rotating and Counter-rotating Mode. *European Conference on Turbomachinery Fluid Dynamics and Thermodynamics, ETC*, 2023. Retrieved from http://dx.doi.org/10.29008/ETC2023-203

20.Zhang, H., Deng, C., Chang, C., You, H. Novel dual synergistic sealing ring design for a high-pressure pump – Part I. Retrieved from http://dx.doi.org/10.12968/s1350-4789(22)70085-2

21.Zhang, H., Deng, C., Chang, C., You, H. Novel dual synergistic sealing ring design for a high-pressure pump – Part II. Retrieved from https://doi.org/10.12968/S1350-4789(22)70086-4

22.Kondus, V., Puzik, R., German, V., Panchenko, V., Yakhnenko, S. (2021). Improving the efficiency of the operating process of high specific speed torque-flow pumps by upgrading the flowing part design. *Journal of Process Mechanical Engineering*, Vol. 237, pp. 1741 012023 https://doi.org/10.1088/1742-6596/1741/1/012023

23.Kondus, V.; Kotenko A. (2017). Investigation of the impact of the geometric dimensions of the impeller on the torque flow pump characteristics. *Eastern-European Journal of Enterprise Technologies*, Vol. 1/4 (88), pp. 25–31. Retrieved from https://doi.org/10.15587/1729-4061.2017.107112

24.Rogovyi, A., Korohodskyi, V., Neskorozhenyi, A., Hrechka, I., Khovanskyi, S., Reduction of Granular Material Losses in a Vortex Chamber Supercharger Drainage Channel. *Advances in Design, Simulation and Manufacturing V. DSMIE 2022. Lecture Notes in Mechanical Engineering*, pp. 218–226. Retrieved from https://doi.org/10.1007/978-3-031-06044-1–21

Reviewer: Oleksandr Ivchenko, Acting vice-rector for scientific and international activities of the Sumy National Agrarian University, Ph.D., associate professor Head of the Department of technical systems design.

© В. Ю. Кондусь